Characterization of Upper-Troposphere Water Vapor Measurements during AFWEX Using LASE

R. A. FERRARE,[a] E. V. BROWELL,[a] S. ISMAIL,[a] S. A. KOOI,[b] L. H. BRASSEUR,[b] V. G. BRACKETT,[b] M. B. CLAYTON,[b] J. D. W. BARRICK,[a] G. S. DISKIN,[a] J. E. M. GOLDSMITH,[c] B. M. LESHT,[d] J. R. PODOLSKE,[e] G. W. SACHSE,[a] F. J. SCHMIDLIN,[f] D. D. TURNER,[g] D. N. WHITEMAN,[h] D. TOBIN,[i] L. M. MILOSHEVICH,[j] H. E. REVERCOMB,[i] B. B. DEMOZ,[h] AND P. DI GIROLAMO[k]

[a]*NASA Langley Research Center, Hampton, Virginia*
[b]*SAIC/NASA Langley Research Center, Hampton, Virginia*
[c]*Sandia National Laboratories, Livermore, California*
[d]*Argonne National Lab, Argonne, Illinois*
[e]*NASA Ames Research Center, Moffett Field, California*
[f]*NASA Wallops Flight Facility, Wallops Island, Virginia*
[g]*Pacific Northwest National Laboratory, Richland, Washington*
[h]*NASA Goddard Space Flight Center, Greenbelt, Maryland*
[i]*University of Wisconsin—Madison, Madison, Wisconsin*
[j]*National Center for Atmospheric Research, Boulder, Colorado*
[k]*DIFA, Università della Basilicata, Potenza, Italy*

(Manuscript received 28 January 2004, in final form 28 April 2004)

ABSTRACT

Water vapor mass mixing ratio profiles from NASA's Lidar Atmospheric Sensing Experiment (LASE) system acquired during the Atmospheric Radiation Measurement (ARM)–First International Satellite Cloud Climatology Project (ISCCP) Regional Experiment (FIRE) Water Vapor Experiment (AFWEX) are used as a reference to characterize upper-troposphere water vapor (UTWV) measured by ground-based Raman lidars, radiosondes, and in situ aircraft sensors over the Department of Energy (DOE) ARM Southern Great Plains (SGP) site in northern Oklahoma. LASE was deployed from the NASA DC-8 aircraft and measured water vapor over the ARM SGP Central Facility (CF) site during seven flights between 27 November and 10 December 2000. Initially, the DOE ARM SGP Cloud and Radiation Testbed (CART) Raman lidar (CARL) UTWV profiles were about 5%–7% wetter than LASE in the upper troposphere, and the Vaisala RS80-H radiosonde profiles were about 10% drier than LASE between 8 and 12 km. Scaling the Vaisala water vapor profiles to match the precipitable water vapor (PWV) measured by the ARM SGP microwave radiometer (MWR) did not change these results significantly. By accounting for an overlap correction of the CARL water vapor profiles and by employing schemes designed to correct the Vaisala RS80-H calibration method and account for the time response of the Vaisala RS80-H water vapor sensor, the average differences between the CARL and Vaisala radiosonde upper-troposphere water vapor profiles are reduced to about 5%, which is within the ARM goal of mean differences of less than 10%. The LASE and DC-8 in situ diode laser hygrometer (DLH) UTWV measurements generally agreed to within about 3%–4%. The DC-8 in situ frost point cryogenic hygrometer and Snow White chilled-mirror measurements were drier than the LASE, Raman lidars, and corrected Vaisala RS80H measurements by about 10%–25% and 10%–15%, respectively. Sippican (formerly VIZ Manufacturing) carbon hygristor radiosondes exhibited large variabilities and poor agreement with the other measurements. PWV derived from the LASE profiles agreed to within about 3% on average with PWV derived from the ARM SGP microwave radiometer. The agreement between the LASE and MWR PWV and the LASE and CARL UTWV measurements supports the hypotheses that MWR measurements of the 22-GHz water vapor line can accurately constrain the total water vapor amount and that the CART Raman lidar, when calibrated using the MWR PWV, can provide an accurate, stable reference for characterizing upper-troposphere water vapor.

1. Introduction

Improving the parameterization of radiative processes in general circulation models (GCMs), which is a primary objective of the Department of Energy (DOE) Atmospheric Radiation Measurement (ARM) Program, requires an accurate specification of the atmospheric state. Measurements of water vapor are especially important for characterizing the atmospheric state because uncertainties in the water vapor field dominate the spectral effects in the atmospheric window region of 800–

Corresponding author address: Richard Ferrare, NASA Langley Research Center, Mail Stop 401A, Hampton, VA 23681.
E-mail: richard.a.ferrare@nasa.gov

1200 cm^{-1} (8.3–12.5 μm) (DOE 1990). Water vapor measurements are also essential for evaluating the strength and formulation of the water vapor continuum absorption. Computing the absorption associated with the continuum is particularly important for computing radiative transfer, which in turn impacts remote sensing retrievals of temperature, water vapor, and surface properties. The strong absorption due to the water vapor pure rotation band (100–400 cm^{-1}) is the principal contribution to the clear-sky upper-troposphere cooling rate (Clough et al. 1992). In addition to directly affecting the atmospheric cooling rate, upper-tropospheric water vapor has a strong indirect effect on the atmospheric radiation budget through its role in the formation and dissipation of cirrus clouds. Uncertainties in radiation budgets of climate models are caused in part by inadequate knowledge of the water vapor fields required to nucleate cirrus ice crystals (Khvorostyanov and Sassen 1998a,b).

Measurements made at the ARM Southern Great Plains (SGP) Cloud and Radiation Testbed (CART) site in northern Oklahoma (36.62°N, 97.5°W) have provided an opportunity to obtain the meteorological and atmospheric radiation data needed to assess radiation models and their use in single-column models (SCMs) and GCMs (Ackerman and Stokes 2003). This site was designed to acquire water vapor data necessary for characterizing the atmospheric state in order to develop and evaluate these models. Operational radiosondes have provided one method for acquiring water vapor profiles, although the required water vapor accuracy ($<$10%) has generally been beyond their measurement capabilities. The Vaisala RS80-H radiosondes launched by ARM were shown to have a dry bias of about 5%–10% (Clough et al. 1996; Turner et al. 2003) as well as considerable variations in their water vapor calibrations (Lesht 1995; Lesht and Liljegren 1996). The dry bias of these radiosondes became particularly apparent at cold temperatures at high altitudes (Miloshevich et al. 2001, 2003, 2004) when compared with satellite (Soden et al. 1994; Soden and Lanzante 1996; Soden et al. 2004) and Raman lidar measurements (Ferrare et al. 1995). Uncertainties in the radiosonde water vapor profiles, which were input to the radiative transfer models, were the limiting factor in comparing measured versus model longwave radiances (Ellingson 1998; Revercomb et al. 1998). These uncertainties also hamper efforts to evaluate upper-tropospheric water vapor measurements acquired by various new satellite sensors.

The difficulty in achieving high accuracy in radiosonde water vapor measurements led ARM to aggressively pursue new technologies for providing the water vapor measurements required for radiation studies. The ARM Program developed the first operational Raman lidar system designed for unattended, around-the-clock atmospheric profiling of water vapor, aerosols, and clouds (Goldsmith et al. 1998). This lidar system measures Raman scattering from water vapor and nitrogen to derive profiles of water vapor mixing ratio. High background skylight limits retrievals of water vapor during daytime operations to altitudes below about 3–4 km so that the Raman lidar upper-tropospheric water vapor measurements are limited to nighttime operations. Comparisons of the Raman lidar and Vaisala radiosonde water vapor profiles have also shown the dry bias and radiosonde variability discussed above. The largest differences between the Raman lidar and radiosonde water vapor profiles are typically found in the upper troposphere, where differences often exceed 20% (Turner and Goldsmith 1999).

The ARM Program has conducted a series of experiments at the SGP site to characterize and ultimately improve the accuracy of water vapor measurements (Revercomb et al. 2003). As the latest in these series of experiments, the ARM–First International Satellite Cloud Climatology Project (ISCCP) Regional Experiment (FIRE) Water Vapor Experiment (AFWEX) was conducted at the SGP site during late November to early December 2000 primarily to characterize the upper-troposphere water vapor (UTWV) measurements acquired at the SGP site. The goal was to develop techniques to reduce uncertainties in UTWV measurements in order to better constrain the top-of-atmosphere (TOA) outgoing longwave (LW) clear-sky flux.

We examined the impact of upper-level water vapor perturbations, or uncertainties, on longwave flux calculations at the TOA. An increase in UTWV causes net radiation to be emitted from higher (and, in general, colder) layers in the atmosphere, which results in a decrease in radiation and flux at the TOA. Similarly, a decrease in UTWV causes an increase in TOA radiance. Since it is primarily the integrated amount of water vapor from the TOA (and the temperature profile) that effects the TOA radiance and flux, water vapor perturbations that are altitude independent above a given lower boundary are examined. Using the Rapid Radiative Transfer Model (RRTM) (Mlawer et al. 1997) to compute LW fluxes and cooling rates, we have computed changes in net flux at the TOA due to perturbations in the UTWV. Figure la shows the change in infrared longwave flux at TOA due to various upper-level water vapor perturbations for the *U.S. Standard Atmosphere, 1976* (NOAA 1976). For a given water vapor perturbation, this figure displays what error would result in the corresponding TOA flux calculation, with all other state variables held fixed. For example, in order to constrain uncertainties in the TOA net flux to less than ~0.5 W m^{-2}, the uppermost 0.1 mm of water vapor must be known to ~10% or better. Figure 2 shows that for AFWEX, the uppermost 0.1 mm of water vapor was typically located between 8 km and the tropopause, which was around 12 km. Figure 1b shows that a 10% increase in water vapor above 8 km reduces the atmospheric heating rates (or increases cooling rates) by over 1 K day^{-1} in portions of the upper troposphere.

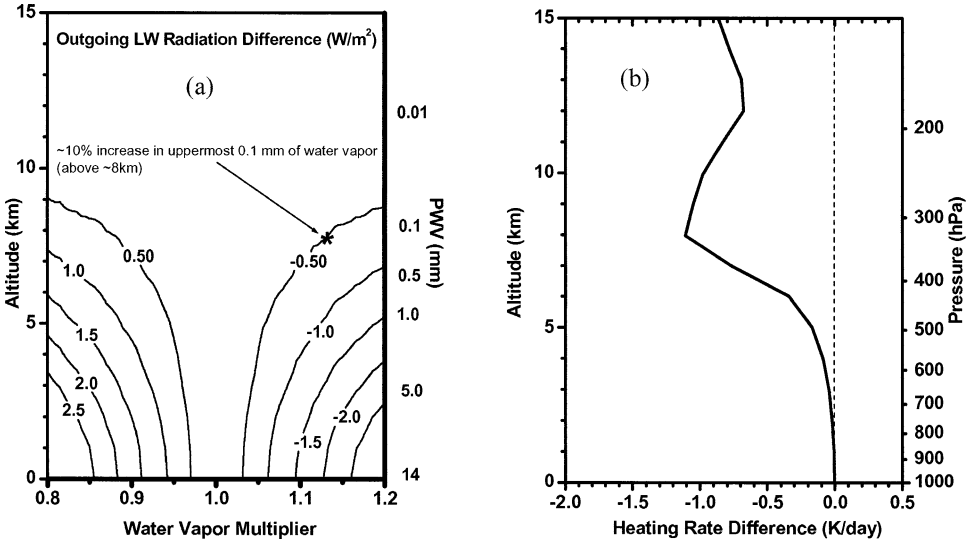

FIG. 1. (a) Difference in TOA outgoing longwave radiation are shown by contours for various perturbations of integrated water vapor amounts above various altitudes. The left-hand ordinate is the lower altitude of perturbation; all water vapor amounts above this altitude are perturbed by the values given in the abscissa. (b) Difference in heating rate profiles for a ~10% increase in water vapor above 8 km. Both (a) and (b) correspond to *U.S. Standard Atmosphere, 1976* conditions.

Additional instruments were deployed specifically during AFWEX to characterize the routine ARM radiosonde and Raman lidar upper-tropospheric water vapor measurements as well as to help resolve absolute water vapor calibration issues impacting total column precipitable water vapor (PWV). One additional instrument was the Lidar Atmospheric Sensing Experiment (LASE) system, which uses the differential absorption lidar (DIAL) technique for high-resolution water vapor and aerosol backscatter profile measurements (Browell and Ismail 1995; Browell et al. 1997). LASE was deployed from the National Aeronautics and Space Administration (NASA) DC-8 aircraft and provided water vapor profiles above and below the aircraft to help characterize UTWV.

In sections 2 and 3 we shall first describe the LASE system and the LASE water vapor measurements acquired during AFWEX. Detailed comparisons of the LASE UTWV measurements with the other AFWEX sensors are presented in section 4. We conclude with a description of the overall comparisons among the AFWEX UTWV measurements and discuss the implications of these UTWV measurements and comparison results.

2. LASE system

LASE is an airborne DIAL system that was developed to measure water vapor, aerosols, and clouds throughout the troposphere (Browell et al. 1997; Moore et al. 1997; Ismail et al. 2000). The laser system of LASE consists of a double-pulsed Ti:sapphire laser that operates in the

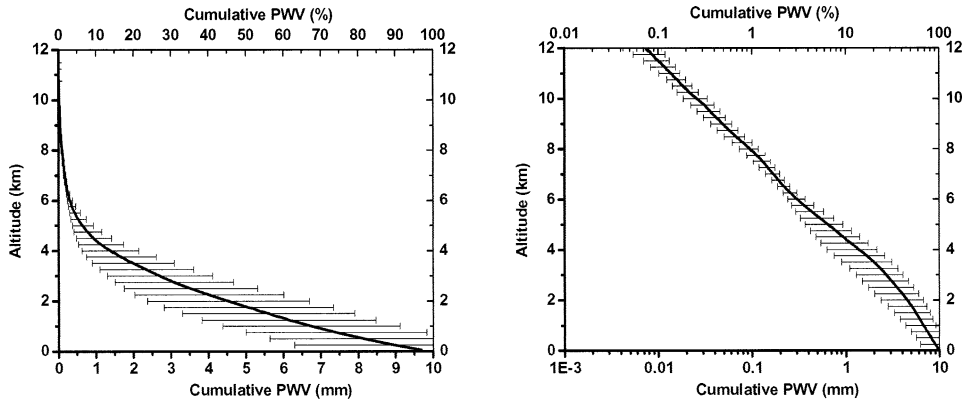

FIG. 2. Mean profile of PWV during AFWEX. Error bars represent std devs. These plots show PWV in both absolute and relative amounts using both (left) linear and (right) logarithmic axes.

815-nm absorption band of water vapor and is pumped by a frequency-doubled flashlamp-pumped Nd:YAG laser. The wavelength of the Ti:sapphire laser is controlled by injection seeding with a diode laser that is frequency locked to a water vapor line using an absorption cell. The laser energy is split using an optical beam splitter and transmitted simultaneously in the nadir and zenith directions. Backscattered lidar signals are received using two telescopes that are aligned to these nadir and zenith directions. Lidar data collected by these telescopes are processed independently. LASE operates by locking to a strong water vapor line and electronically tuning to any spectral position on the absorption line to choose the suitable absorption cross section for optimum measurements over a range of water vapor concentrations in the atmosphere. LASE operates by alternating between strong (line center) and weak (side of strong line) water vapor cross sections for the online DIAL wavelength to measure water vapor throughout the troposphere. In addition, LASE can interleave operation on up to three different online positions to cover the large variation in water vapor concentrations. This unique method of operation permits rapid and flexible absorption cross-section selection capability for water vapor measurements over the entire troposphere in a single pass.

During AFWEX, LASE used two different online positions to measure water throughout the troposphere. For the upper-tropospheric water vapor measurements, LASE used the strongly absorbing temperature-insensitive H_2O line at 817.2231 nm (12 236.5603 cm^{-1}) (Ponsardin and Browell 1997; Ismail et al. 2000), which has a line strength of 4.060E-23 cm, line width of 0.0839 cm^{-1}, and lower energy state of 224.838 cm^{-1}. Ponsardin and Browell (1997) characterized the spectral lines in the 815-nm region used by LASE. These line characterizations were done using a continuous-wave, nearly monochromatic laser source with a line width of about 10^{-4} cm^{-1}, and these measurements took into account the line-broadening and narrowing effects, pressure shifts, and temperature dependencies. Grossmann and Browell (1989) estimated the uncertainties in the line strengths of $\sim$2% and line widths of $\sim$1.5%, giving a total (rms) uncertainty of $<$3% for the absorption cross section. Recent measurements using Fourier transform infrared (FTIR) techniques (Schermaul et al. 2001) show that they agree well with Grossmann and Browell (1989) and Ponsardin and Browell (1997) to within 2%–3%. The centerline and offline combination and sideline and offline combination were used for water vapor measurements in the range $<$0.01 to 1 g kg^{-1} and 0.5 to 10 g kg^{-1}, respectively. Lidar data are averaged by applying vertical smoothing and shot averaging to limit the random error to be in the range of 2%–5%. LASE is operated to minimize systematic errors arising from uncertainties in the laser spectral characteristics, knowledge of molecular water vapor absorption cross section, and atmospheric influences (Ismail and Browell 1989). All known systematic effects are corrected, and the combined residual systematic errors are expected to be in the range of 3%–5%. The estimated total accuracy of LASE is expected to be in the range of 5%–10%. Effective absorption cross-section profiles were calculated at the on- and offline wavelengths using the methods discussed by Ismail and Browell (1989) for the calculation of water vapor concentrations using the DIAL equation (Shotland 1966; Browell 1989). For AFWEX, absolute water vapor distributions were derived from the LASE measurements across the entire troposphere from 0 to 12 km over a mixing ratio range of 10–0.01 g kg^{-1}. The LASE nadir water vapor profiles have a vertical resolution of about 330 m for altitudes above 330 m above ground level (AGL). The range cell size was decreased from 330 to 150 m for altitudes below 330 m in order to extend the LASE profiles down to within about 250 m above the surface. Zenith water vapor profiles have a vertical resolution of about 990 m. The LASE nadir water vapor profiles have a temporal averaging period of 1 min. This corresponds to a horizontal resolution of about 14 km, which is the horizontal distance covered by the DC-8 aircraft during this time. The LASE zenith water vapor profiles are averaged over a period of 5 min, which corresponds to a horizontal distance of about 70 km. LASE also simultaneously measures profiles of aerosol scattering ratio at the offline wavelength near 815 nm. Ismail et al. (2000) describe in detail the methods used to derive aerosol profiles using this offline laser return signal.

During the LASE Validation Experiment (Browell et al. 1997) and Tropospheric Aerosol Radiative Forcing Observation Experiment (TARFOX) (Ismail et al. 2000; Ferrare et al. 2000a,b), LASE operated autonomously from the Q bay of the NASA ER-2 aircraft. During the former experiment, comparisons of the LASE water vapor measurements with in situ water vapor measurements on two additional aircraft (C-130 and Learjet), radiosonde profiles, and the ground-based NASA Goddard Space Flight Center (GSFC) scanning Raman lidar (SRL) water vapor mass mixing ratio profiles showed agreement to be better than 6% or 0.01 g kg^{-1}, whichever is greater throughout the troposphere (Browell et al. 1997). Subsequent to the two LASE missions on the ER-2, it was reconfigured to fly onboard the NASA P-3 and DC-8 aircraft and participated in another seven major field experiments. Once the LASE system was configured for operation from the DC-8 in the simultaneous nadir and zenith modes of operation, additional comparisons were made with other sensors to insure the accuracy of the water vapor measurements. Intercomparisons performed during the third Convection and Moisture Experiment (CAMEX3) (Ferrare et al. 1999; Browell et al. 2000), Pacific Exploratory Mission (PEM) Tropics B (Browell et al. 2001), and CAMEX4 (Kooi et al. 2002) missions produced results consistent with the initial LASE validation experiments.

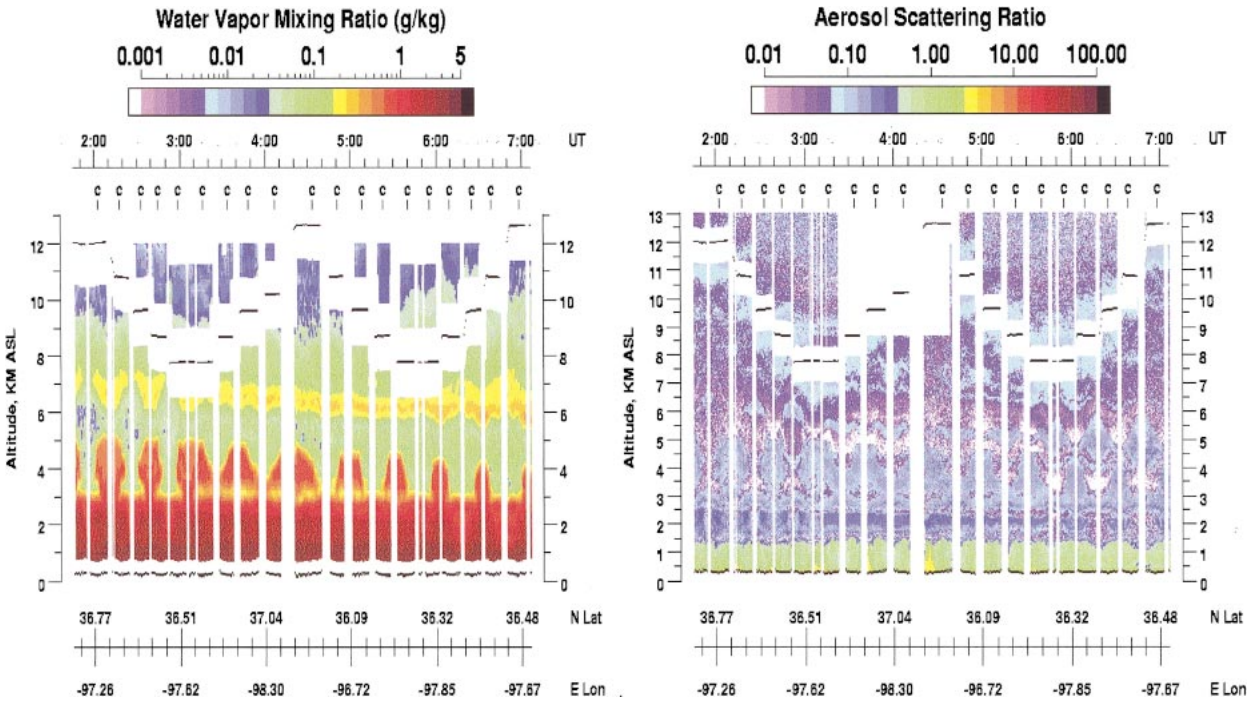

FIG. 3. LASE (left) water vapor and (right) aerosol scattering ratio profiles acquired during AFWEX DC-8 flight 7 on 5 Dec 2000. The aircraft flight altitudes are indicated by the horizontal black lines. The times when the DC-8 flew directly over the ARM SGP Central Facility are denoted by the letter ''c.''

3. LASE measurements during AFWEX

After the transit flight of the DC-8 to Tinker Air Force Base (AFB) (35.4°N, 97.38°W) on 29 November, there were a total of six science flights of the DC-8 over the ARM SGP site between 30 November and 10 December. LASE collected approximately 26 h of data during these flights. The flight patterns typically consisted of a spiral ascent over the SGP site, followed by a series of level leg segments at several different altitudes in the upper troposphere, followed by a spiral down over the SGP site before the DC-8 returned to Tinker AFB. The spiral portions of each flight permitted the DC-8 in situ water vapor sensors to acquire a vertical profile over the SGP site. The level leg segments were performed at several altitudes between about 7.7 and 12.4 km above the SGP site. These segments, which were oriented both parallel and perpendicular to the wind at these altitudes, were approximately 10 min (140 km) in duration and were centered over the ARM SGP site. In order to optimize the airborne and ground-based lidar measurements, flights were conducted during generally clear skies or when only thin cirrus clouds were present. Consequently, the flights occurred after the fronts and associated clouds passed the SGP site. During those nights when flights occurred, winds in the upper troposphere were generally from the northwest or west-northwest. Also, during these flights when skies were clear or partly cloudy, the polar jet stream was generally located north of this region. Inspection of the AFWEX water vapor profiles shows that they often contained deep moist layers in the upper troposphere (RH $>$ 40%).

Figure 3 shows examples of LASE water vapor and aerosol scattering ratio profiles for flight 7 on 5 December 2000. Because of near-field signal effects associated with the incomplete overlap of the laser beam and telescope field of view, LASE cannot retrieve water vapor profiles within about 1 km above and below the aircraft. On this night, skies were cloud-free over northern Oklahoma, with generally northwesterly flow above 8 km. Geostationary Operational Environmental Satellite (GOES) water vapor imagery showed that drier conditions existed toward the northeast, where a high pressure center was located over Iowa. During the first part of this flight, until about 0330 UTC, and during the latter part of the flight, after 0550 UTC, the DC-8 flew a series of level flight legs oriented approximately northeast–southwest. This orientation was along the gradient of water vapor and was perpendicular to the wind direction. Between 0330 and 0550 UTC, the LASE flew legs oriented nearly parallel to the wind and perpendicular to the water vapor gradient. The increase in aerosol scattering below about 2 km can be seen in these images. For AFWEX, the LASE water vapor profiles were derived for altitudes below 12 km. Temperature profiles from the DOE ARM SGP radiosondes, as well as in situ ozone measurements on board the NASA DC-8, indicated that tropopause altitudes varied between 10 and 12 km during the DC-8 flights in AFWEX. Figure

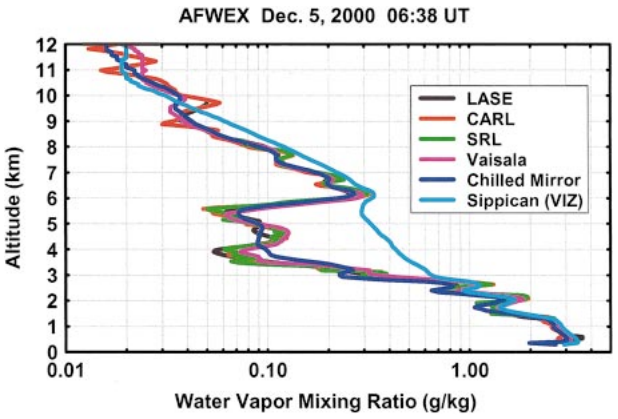

FIG. 4. A comparison of water vapor profiles acquired at around 0638 UTC 5 Dec 2000.

4 shows an example comparison at 0638 UTC on 5 December 2000 among several water vapor profiles acquired during this flight. The CART Raman lidar (CARL) and SRL profiles correspond to 10-min average profiles and the LASE profile corresponds to a 2-min average centered over the SGP site. With the exception of the Sippican radiosonde profile, there was generally good agreement among these profiles, although small differences of a few percent are not easily seen when plotted on a semilogarithmic scale. The reason for the significant dry layer between 3 and 5 km is not clear. In situ ozone measurements on the DC-8 did not show any significant increase in ozone in this region, so this layer does not appear to be the direct result of a tropopause fold. Comparisons of water vapor measurements will be examined in greater detail in the next section.

4. LASE water vapor comparisons during AFWEX

Water vapor measurements acquired by two ground-based Raman lidars (CARL and SRL), three radiosonde sensors [Vaisala RS80-H, Sippican Inc. (formerly VIZ Manufacturing Company) carbon hygristor, Snow White chilled mirror], and two DC-8 in situ sensors [NASA Langley/Ames diode laser hygrometer (DLH), cryogenic frost point hygrometer] were compared with the LASE profiles. The Sippican and chilled-mirror radiosonde sensors were carried aloft together on the same balloon, and the Vaisala radiosondes were launched separately. Table 1 lists the number of individual comparisons performed with each of the profile and in situ measurements during each DC-8 flight. The number of individual comparisons with the various sensors varied from 46 (CARL) to 16 (chilled-mirror and Sippican sondes). These comparisons included profiles that were acquired within 30 min of LASE profiles and when the DC-8 was within about 30 km of the ARM SGP site. For the comparisons that follow, we examined profiles of water vapor mixing ratio, which are the normal output products of LASE, the Raman lidars, and the in situ diode laser hygrometer. Thirty-minute-average profiles from the two Raman lidars were compared with the UTWV measurements from LASE. With the exception of the Vaisala profiles, the radiosonde profiles of relative humidity and the chilled-mirror measurements of dew/frost point temperature were converted to water vapor mixing ratio using the Goff–Gratch formulas of vapor pressure over liquid water (Goff and Gratch 1946; List 1984). Vaisala uses the Hyland–Wexler (Hyland and Wexler 1983) formulas to derive vapor pressures. Differences between these two formulations can lead to significant differences in the derived vapor pressures for cold temperatures in the upper troposphere (Miloshevich et al. 2001). For AFWEX, water vapor comparisons were performed for altitudes below 12 km, where nearly all temperatures were warmer than −60°C. In this case, our computations show that differences in the water vapor mixing ratios computed using these two vapor pressure formulations are less than 3%. Average differences discussed in section 5 change by less than 1% when computed using these two vapor pressure formulations. Uncertainties in the radiosonde temperature measurements may introduce an additional error in the computation of water vapor mixing ratio from relative humidity. Operational experience at the SGP CART site (Lesht 1995) showed that the rms error in the Vaisala temperature measurements was approximately 0.3°C.

TABLE 1. Number of individual comparisons from each sensor with LASE water vapor measurements. The numbers corresponding to the Raman lidar and radiosonde comparisons represent profile comparisons, and the DLH and cryogenic hygrometer numbers represent the number of comparisons from averages acquired during level legs.

Sensor	28 Nov	30 Nov	4 Dec	5 Dec	7 Dec	9 Dec	10 Dec	Total
CARL	3	5	0	10	9	10	9	46
SRL	0	0	0	10	0	10	9	29
Vaisala sonde	1	3	2	6	2	2	5	21
Chilled-mirror sonde	0	3	0	4	2	3	4	16
Sippican sonde	0	3	0	4	2	3	4	16
DLH	0	11	0	24	10	19	17	81
Cryogenic hygrometer	0	11	0	24	10	19	0	64

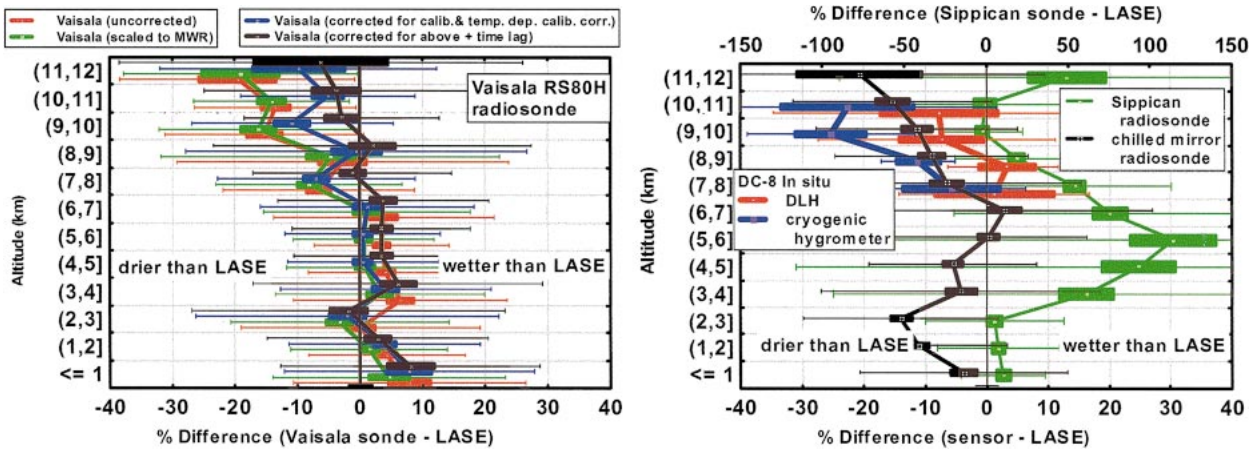

FIG. 5. (a) Average differences between LASE and Vaisala water vapor measurements. The thick rectangles (boxes) represent ±2 SE of the mean, and error bars represent ±1 std dev of the measurements. Differences between any two categories are statistically insignificant when the ±2 SE boxes overlap. Average differences between LASE water vapor measurements and the uncorrected Vaisala profiles, Vaisala profiles scaled to match the MWR PWV, Vaisala profiles corrected for calibration errors, and Vaisala profiles corrected for both calibration errors and time-lag response are shown. (b) Average differences between the LASE and chilled-mirror and Sippican radiosonde profiles, and the DLH and cryogenic hygrometer in situ instruments on the DC-8. The top axis corresponds to the Sippican radiosonde, and the bottom axis corresponds to the other instruments.

This error would lead to an uncertainty of about 3%–4% in water vapor mixing ratio for altitudes between 8 and 12 km.

a. Vaisala RS80-H radiosondes

Radiosondes have been the most requested operational source of water vapor profile information for the ARM SGP site. Consequently, the LASE water vapor measurements were used first to examine the radiosonde water vapor mixing ratio profile. Figure 5a shows the average difference (%) between the LASE and the Vaisala RS80-H water vapor mixing ratio values as a function of altitude. Differences were computed every 60 m along these profiles; average differences were then computed for 1-km segments, shown in Fig. 5. For these computations, the radiosonde profiles were smoothed to match the vertical resolution (330 m) of the LASE profiles. This smoothing should significantly reduce random errors for scales below 1 km. The thick rectangles (boxes) represent ±2 standard error (SE) of the mean, and bars represent ±1 standard deviation of the measurements. Differences between any two categories are statistically insignificant when the ±2 SE boxes overlap. Average differences were generally below 10% for altitudes below 8 km, which is consistent with comparisons of radiosonde and Raman lidar profiles during the 1996 and 1997 Water Vapor IOPs (Turner and Goldsmith 1999; Revercomb et al. 2003). Above 8 km, radiosonde water vapor profiles were progressively drier than the LASE profiles, with average differences of about 20% for altitudes above about 11 km. This upper-troposphere dry bias of the Vaisala RS80-H radiosonde is also consistent with previous comparisons with CART Raman lidar profiles (Turner and Goldsmith 1999).

In an effort to reduce the radiosonde bias and variability, ARM has pursued methods of correcting the water vapor profiles measured by the Vaisala RS80-H radiosondes. One method applies a single, altitude-independent scaling factor to the radiosonde water vapor measurements such that the column precipitable water vapor (PWV) computed from the resulting radiosonde water vapor matches simultaneous microwave radiometer (MWR) PWV measurements (Turner et al. 2003). The radiosonde water vapor mixing ratio profile is scaled by the ratio of the MWR PWV to the radiosonde PWV. Since the radiosonde PWV is generally less than the MWR PWV, these scale factors generally range from 1.0 to 1.1 (Revercomb et al. 2003; Turner et al. 2003). This method assumes that the MWR PWV is a stable and accurate reference, and that the scaling factor is independent of altitude. The excellent stability and sensitivity of the MWR is supported by several years of MWR results and intercomparisons with other microwave radiometers (Liljegren 2000; Revercomb et al. 2003) as well as by comparisons performed with SRL data adjusted to match calibrated chilled-mirror sensors on the 60-m instrumented tower at the SGP site (Revercomb et al. 2003). While the agreement between the chilled-mirror-calibrated SRL and MWR PWV showed a slope of 0.996, the offset translated into a 3%–4% difference, with the chilled-mirror-calibrated SRL slightly drier (Revercomb et al. 2003). The reasons for this difference are not understood and are under investigation.

In previous studies, scaling the radiosonde water vapor profiles to match the MWR PWV reduced by a factor of 2 the rms differences between the spectral radiances measured by the atmospheric emitted radiance interferometer (AERI) and those produced by the line-by-line

radiative transfer model (LBLRTM) so that this scaling significantly reduced the variability in the radiosonde moisture profiles (Clough et al. 1999; Turner et al. 2004). However, Fig. 5a shows that this scaling had a minimal impact on the radiosonde upper-troposphere water vapor profiles that were coincident to the LASE measurements. This result is not surprising for two reasons. First, the average MWR scaled correction for these 16 radiosonde profiles was 0.98 so that, for at least these sondes, the average sonde PWV was actually slightly greater than the MWR PWV. Second, Fig. 5a shows that the differences between the LASE and radiosonde profiles differ with altitude, so that a correction based primarily on radiosonde performance in the lower troposphere will not have the same impact on upper-tropospheric measurements.

A second series of correction schemes has been developed to account for the variability and dry bias of the Vaisala RS80-H measurements. These schemes generally account for two sources of error: ''bias'' errors that produce a dry bias in the measurements and a ''time lag'' error that results from a slow response of the sensor to a changing ambient relative humidity field at cold temperatures (Miloshevich et al. 2002). A joint effort between Vaisala and the National Center for Atmospheric Research (NCAR) has produced a scheme that includes bias-error corrections for chemical contamination, temperature-dependence, basic-calibration-model, ground-check, sensor-aging, and sensor-arm-heating errors (Wang 2002; Wang et al. 2002). The major sources of bias error are due to the first three items listed above. Initial studies have indicated that these corrections have led to a better (Wang 2002), but still not acceptable (Wang et al. 2003), agreement in the upper-tropospheric humidity (UTH) between the RS80 data and other independent measurements. Comparisons of PWV measurements acquired over many years show that this bias correction moistens the radiosonde profiles and produces excellent agreement between the corrected radiosondes and MWR in absolute amount (Turner et al. 2003). Portions of this correction scheme were applied to the AFWEX data to account for the error in the basic RS80-H calibration model and to improve the representation of the temperature dependence of the RS80-H calibration. The AFWEX sondes were recently manufactured, so no correction was applied to account for possible sensor contamination by outgassing of the plastic packaging material. Figure 5a shows that this temperature-dependence and calibration-model correction does moisten the Vaisala water vapor profiles in the upper troposphere and brings these into closer agreement to the LASE measurements, reducing average differences from about 18%–20% to 8%–10%. This correction has a minimal impact on radiosonde water vapor measurements below about 7 km.

A correction for the time-lag error has also been developed that calculates the ambient humidity profile from the measured humidity and temperature profiles based on laboratory measurements of the sensor time constant as a function of temperature (Miloshevich et al. 2001, 2002, 2003, 2004). The time constant is the time required for the sensor to respond to 63% of a change in humidity. This correction has been evaluated using simultaneous relative humidity measurements from the National Oceanic and Atmospheric Administration/Climate Modeling and Diagnostics Laboratory (NOAA/CMDL) balloon-borne frost point hygrometer. Preliminary comparisons of uncorrected radiosonde profiles and profiles corrected for both the bias and time-lag error corrections have been done for the AFWEX measurements (Miloshevich et al. 2002, 2003, 2004). These preliminary results indicate that, when compared to the uncorrected radiosonde profiles, the temperature-dependence and calibration-model correction moistens the radiosonde upper-tropospheric water vapor profiles by about 10% on average. Similar comparisons also show that the time-lag correction also tends to moisten the UTWV measurements by a few percent and significantly decreases the water vapor measurements in the lower stratosphere. Figure 5a shows that this correction also tends to moisten the AFWEX Vaisala radiosondes and further reduces the average differences from about 8%–10% to about 4%–5% and, consequently, were within the goal of 10% in mean differences in UTWV. As shown in Fig. 1, the errors in TOA outgoing LW flux that would result from this remaining 4%–5% dry bias in the Vaisala water vapor profiles would be less than about 0.3 W m^{-2}. Corresponding errors in the atmospheric heating rates should be less than about 0.5 K day^{-1}. These results indicate that these bias and time-lag corrections should be applied to the Vaisala radiosonde data before using these data to quantitatively study upper-tropospheric water vapor.

b. Sippican radiosondes

LASE water vapor profiles were also compared with water vapor profiles measured by two additional radiosonde water vapor sensors. The first was a Sippican Mark II Microsonde carbon hygristor radiosonde, similar to that used by the National Weather Service (NWS) at many stations. (As of 1 June 1998, the NWS uses Vaisala RS80-H at 60 of its network stations and Sippican radiosondes in the remaining 32 stations.) Figure 5b shows a comparison of the average differences between the LASE and Sippican profiles. Note the change in scale from the previous plots. The Sippican profiles exhibited erratic performance at low relative humidity. The relatively smooth nature of the Sippican profiles suggests that these carbon hygristor sensors have a long time response and/or become nonresponsive at cold temperatures and/or low water vapor amounts. Results from the World Meteorological Organisation (WMO) Global Positioning System (GPS) Radiosonde Intercomparison campaign held in Brazil during May and June 2001 also showed that the Sippican sensors overestimated relative

humidity values when compared to other sensors and had large rms differences (da Silveira et al. 2003). These comparisons also found that the Sippican measurements reported relative humidity values 5%–10% higher than the Snow White chilled-mirror sensors for low (<20%) relative humidity cases and found that the Sippican measurements were not reproducible at low humidity (Smout et al. 2002). Comparisons between the Snow White chilled-mirror sensor and the Sippican radiosonde during the International H_2O Project 2002 (IHOP_2002), which was held during May and June 2002 over the Southern Great Plains in the United States, found that the Sippican carbon hygristor sensor failed to respond to humidity changes in the middle and upper troposphere (Wang et al. 2003).

c. Meteolabor Snow White radiosondes

Water vapor profiles measured by the Meteolabor Snow White (SW) chilled-mirror dewpoint hygrometer were also compared to the LASE profiles. This sensor measures the dewpoint (or frost point) by measuring the temperature at which the onset of condensation occurs on a mirror. The mirror is maintained at a constant reflectivity by continuously adjusting the mirror temperature. The accuracy of the mirror temperature measurement is less than 0.1 K, and the SW response time is negligible at 20°C, 10 s at −30°C, and 80 s at −60°C (Wang et al. 2003). The SW sensor needs no individual external calibration. Studies done to characterize the SW characteristics indicate that it could be used as a possible reference in the upper troposphere (Fujiwara et al. 2003; Wang 2002; Wang et al. 2003). In the case of the AFWEX comparisons, Fig. 5b shows that the Snow White sensors were progressively drier than the LASE profiles above about 7–8 km. The reason for these differences is not clear but may be related to limitations of the Snow White sensor under very cold, dry conditions. Vömel et al. (2003) examined the behavior of the Snow White chilled-mirror hygrometer under dry conditions using simultaneous humidity measurements from the NOAA/CMDL frost point hygrometer. While these comparisons showed generally good performance, some limitations of this device impact upper-tropospheric water vapor measurements. These limitations were associated with the cooling efficiency of the Peltier cooler and the sensitivity of the frost layer detection. Comparisons with the cryogenic frost point hygrometer were complicated and did not allow for a clear characterization. In some cases, differences could be explained by dry layers, which caused the Snow White sensor to be biased low or high within such layers and, at times, above these layers. The WMO Intercomparison Campaign found that, at temperatures colder than −50°C, a modification introduced by the manufacturer caused instability in the Snow White output, so this sensor could not be used as a reference at these temperatures (da Silveira et al. 2003). For temperatures between −50° and −25°C, the Snow White sensor was considerably wetter than the Vaisala RS90 and RS80 sensors, with average RH differences of 5%–40%. Comparisons of Snow White radiosondes, Vaisala RS80, RS90, and RS93 dropsondes were performed during the Measurement of Tropospheric Humidity (MOTH) Tropic and Arctic field experiments (Vance et al. 2004). These results indicated that the Snow White sensors had a wet bias at both high and low water vapor mixing ratios. These biases were believed to be largely due to the heater on board the Snow White being unable to fully clear the mirror at cold upper levels and at low levels during hot, humid conditions (Vance et al. 2004).

d. Raman lidars

The requirement for frequent, high-vertical-resolution water vapor profiles led ARM to develop the first operational Raman lidar system designed for unattended, around-the-clock atmospheric profiling of water vapor, aerosols, and clouds (Goldsmith et al. 1998). This lidar system measures Raman scattering from water vapor and nitrogen to derive profiles of water vapor mixing ratio. A narrow field of view and narrowband filter system reduces the solar background skylight during the day, so that this system can measure water vapor profiles during both daytime and nighttime operations. However, since profiles of water vapor above 3–4 km are limited to nighttime operations, the Raman lidar data acquired during AFWEX discussed here are limited to nighttime operations. Derived products from the CARL measurements include water vapor mixing ratio, aerosol scattering ratio, backscatter coefficient, depolarization and extinction, and cloud optical depth.

The NASA GSFC SRL is a mobile system contained in a single environmentally controlled trailer. For the AFWEX experiment, the SRL used a 9-W, 30-Hz Nd:YAG laser, a 0.76-m telescope, and a large-aperture scanning mirror to make its measurements. Using Raman scattering from atmospheric molecules, the SRL measures water vapor, nitrogen, liquid water, aerosol depolarization, and Rayleigh–Mie signals. The products derived from the SRL measurements include those products listed above for CARL as well as cloud liquid water. Whiteman and Melfi (1999) and Whiteman et al. (2001a,b) provide a more complete description of the SRL. Prior to AFWEX, the SRL received several technology upgrades that improved its UTWV measurement capability. The new technologies deployed to the SGP site for this campaign included narrower-bandwidth filters and data acquisition devices permitting stronger signals to be sampled while using the high-energy/pulse Nd:YAG laser.

Calibration of Raman lidar water vapor profiles is normally achieved by comparisons to other independent water vapor measurements such as water vapor profiles from radiosondes (Ansmann et al. 1992; Ferrare et al. 1995), in situ water vapor measurements from a col-

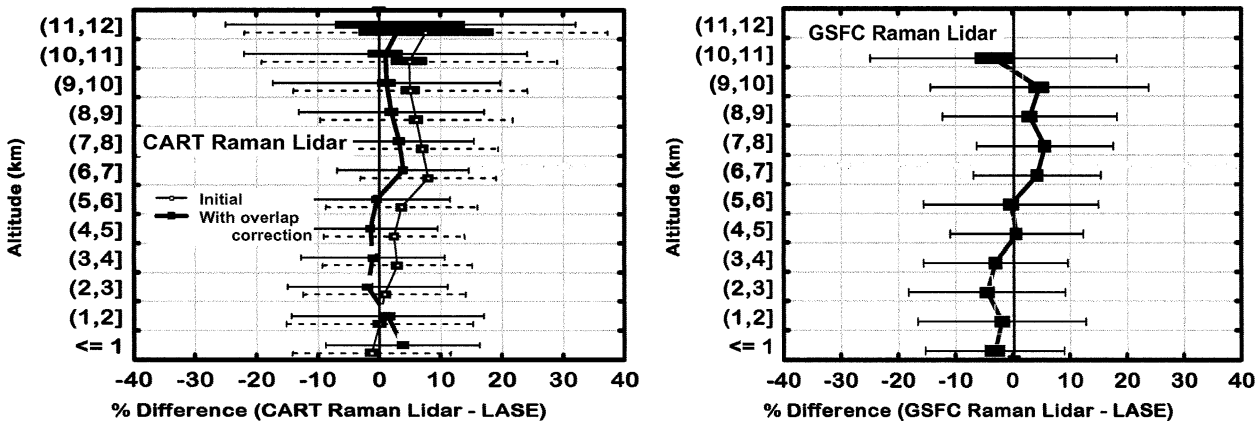

FIG. 6. (a) Average differences between LASE and CARL water vapor measurements. Average differences between LASE water vapor measurements and the uncorrected CARL profiles and the CARL profiles with the overlap correction applied. (b) Average differences between the LASE and SRL profiles.

located tower (Turner et al. 2002), or precipitable water vapor measured by a microwave radiometer (Turner and Goldsmith 1999; Turner et al. 2002) or GPS (Whiteman et al. 2002). Sherlock et al. (1999) describe an absolute calibration technique that does not rely on external water vapor measurements and show that the total absolute uncertainty in the calibration determined from this technique is about 12%–14%. Whiteman et al. (2001b) describe a calibration technique that relies on using the SRL water vapor measurements acquired just below the bases of small cumulus clouds, where the saturation mixing ratio is known from coincident temperature and pressure profiles obtained from radiosondes. The average calibration coefficient derived from this technique agreed to within 1% of the average calibration coefficient derived by comparing water vapor profiles with coincident Vaisala RS80-H radiosondes. The Raman lidar data acquired during AFWEX that are discussed here were calibrated in a manner similar to that described for the MWR scaled radiosonde profiles, such that the total column water vapor from the Raman lidar matches the MWR PWV.

Average differences between the LASE water vapor profiles and the profiles measured by CARL and the SRL were computed as a function of altitude. Figure 6a shows the average difference (%) between the LASE and the CARL water vapor mixing ratio values as a function of altitude. Figure 6b shows a similar comparison between LASE and NASA GSFC scanning Raman lidar. The thick rectangles (boxes) represent ± 2 SE of the mean, and error bars represent ± 1 standard deviation of the measurements. The LASE and the Raman lidar profiles generally agreed on average within 10% for all altitudes. The initial, uncorrected CARL profiles were about 5%–8% wetter than LASE for altitudes above 7 km.

The differences between LASE and CARL were examined more closely. The assumption that the Raman lidar water vapor calibration is height independent requires that the near-field overlap correction must also be known accurately. This overlap correction (Whiteman et al. 1992), which affects profiles below 800 m, is determined directly from the calibration data (Goldsmith et al. 1998; Turner and Goldsmith 1999). The impact of this overlap correction has been checked by comparisons with various sensors. Comparisons of water vapor profiles from chilled-mirror sensors flown on tethered balloons during the Water Vapor IOPs conducted in 1996 and 1997 (Turner et al. 2003) and with the data acquired by the NASA GSFC SRL system during these experiments (Revercomb et al. 2003) suggest that the overlap function can be determined very well. However, comparisons of water vapor profiles acquired during September and October 2000 by these two Raman lidars showed the ARM Raman lidar to be systematically drier than the SRL by 4%–8% below 800 m; above this altitude, the systems showed better agreement (Whiteman et al. 2002). Additional comparisons showed the CARL water vapor measurements at 60 m to be about 8% drier than those from a collocated tower sensor. These recent results, which imply that the overlap function for the ARM Raman lidar was in error, indicate that water vapor profiles calibrated using a single, height-independent calibration constant determined from the MWR PWV would be in error.

We developed a correction to the Raman lidar profiles acquired during AFWEX to account for this error in the overlap function. To determine this correction, we used the MWR-scaled Vaisala radiosonde water vapor profiles to examine the altitude dependence of the CARL water vapor profiles. Since both the CARL and the MWR-scaled Vaisala profiles are scaled to match the MWR PWV, we assume that any differences between the CARL and MWR-scaled Vaisala profiles *within the lowest 2 km* are due to errors in the CARL overlap corrections. Figure 7a shows the average difference between the CARL and MWR-scaled Vaisala radiosonde profiles during AFWEX. Figure 7a shows that CARL

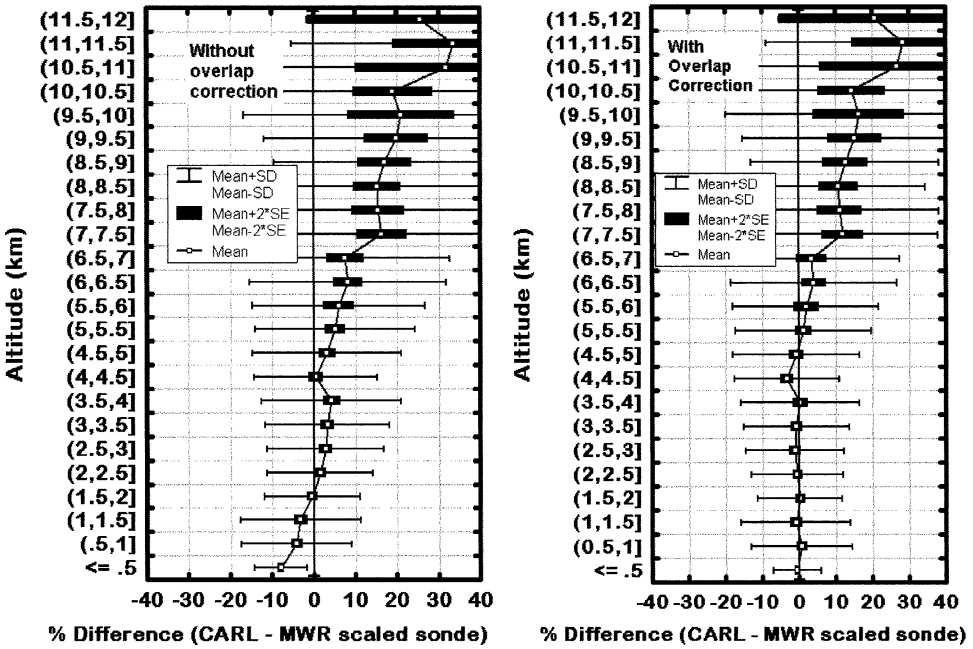

FIG. 7. (a) Average difference between CARL water vapor profiles and the Vaisala water vapor profiles that were scaled to match the MWR PWV. (b) Same as (a) except the overlap correction was applied to the CARL profiles.

profiles are on average drier than the MWR-scaled Vaisala profiles for altitudes below 2 km. These average differences were greatest near the surface (~8%) and gradually decreased to near 0% around 2–3 km. Above 2–3 km, the CARL profiles gradually became wetter than the MWR-scaled Vaisala sondes. Therefore, although the CARL profiles are scaled to match the MWR PWV, when compared to the MWR-scaled Vaisala profiles, the uncorrected CARL profiles have systematically too little water vapor in the lowest few kilometers and too much water vapor in the upper troposphere. An altitude-dependent correction to the CARL profiles was applied such that the average CARL/MWR-scaled Vaisala ratio profile was equal to unity for altitudes below 2.5 km. In order for the resulting PWV to remain in agreement to the MWR PWV, Fig. 7b shows that this correction had the effect of adding water vapor in the lowest 2.5 km and reducing water vapor above 2.5 km. On average, this correction increased the CARL profiles by about 4% below 2.5 km and decreased the CARL profiles by about 4% above 2.5 km. Figure 6a shows that this correction reduced the differences between the CARL and LASE profiles such that the CARL profiles were, on average, less than 5% wetter than the LASE profiles. Note that this correction has only been applied to this AFWEX dataset. Therefore, these results indicate that the CARL profiles should be periodically compared with the MWR-scaled radiosonde profiles in the lowest few kilometers to determine whether additional corrections are necessary.

An additional factor must be considered when assessing the altitude dependence of the Raman lidar water vapor calibration. Since these lidars use very narrow bandwidth filters to reduce background skylight, the change in the Raman spectrum of water vapor with temperature must be considered (Whiteman 2003a, b). For a narrow bandpass filter, the integrated intensity of the Raman scattering feature across the water vapor scattering band will be temperature sensitive. Recent modeling has indicated that this change in sensitivity can lead to errors of several percent in water vapor mixing ratio when comparing Raman lidar water vapor return signals between warm temperatures at low altitudes and cold temperatures at high altitudes. Preliminary modeling suggests that the upper-tropospheric water vapor profiles from the CART Raman and NASA GSFC scanning Raman lidars should be reduced by about 4% (Whiteman et al. 2002; Ferrare et al. 2002). However, more recent modeling has indicated that this temperature sensitivity is highly dependent on having exact knowledge of the filter characteristics (e.g., central wavelength and filter width) so that the impact of this correction is still somewhat uncertain (Whiteman 2003b). The relatively good agreement between the LASE and CARL profiles shown in Fig. 6 suggests that the impact of temperature sensitivity effect should be small (<5%).

The excellent agreement among the Raman lidars, which were calibrated using the MWR PWV, and LASE measurements indicates that the LASE absolute water vapor calibration agrees well with the MWR absolute water vapor calibration. We verified this observation by comparing PWV derived from the LASE water vapor

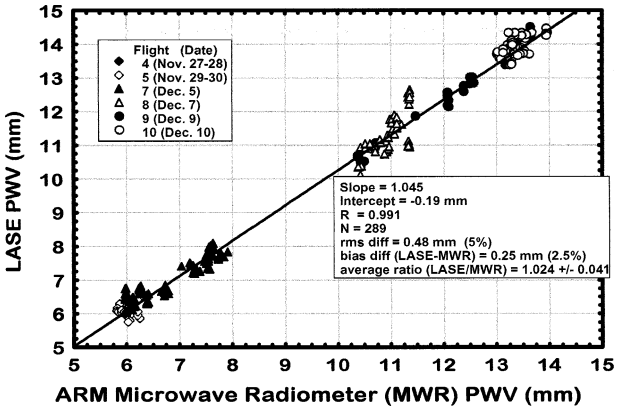

FIG. 8. Comparison of PWV derived from the SGP MWR measurements and the LASE water vapor profiles.

profiles with the MWR PWV. Figure 8 shows a comparison of the PWV derived from the LASE and PWV measurements. When deriving PWV from the LASE profiles, two different methods were used to estimate the small (~10%) contribution to the PWV for altitudes between the surface and the lowest LASE water vapor measurement about 250 m above the surface. The first method interpolated through this region using the LASE water vapor profile above 250 m and the water vapor measurements measured at 25 and 60 m by Vaisala Humicap capacitive relative humidity sensors on the 60-m tower at the ARM SGP facility. The second method used an average of the LASE water vapor measurements between 250 and 400 m above the surface as an estimate of the average water vapor below 250 m. The average PWVs computed from the LASE profiles using these two methods were within 0.25% of each other and were only slightly higher (<3%) than the MWR PWV. The average percentage difference between the LASE and MWR PWV increases slightly with PWV; this small increase does not appear to be related to the vertical distribution of water vapor.

e. DC-8 in situ sensors

Water vapor measurements acquired by in situ sensors on the DC-8 were also compared with the LASE measurements. Two different in situ sensors were examined: the NASA Langley/Ames diode laser hygrometer (DLH) and the NASA Langley cryogenic hygrometer. The in situ water vapor measurements acquired by these instruments during level leg flights were averaged together and compared with the LASE nadir (zenith) water vapor measurements acquired when the DC-8 flew at a higher (lower) altitude either just before or after the in situ measurements. These results were averaged together in 1-km-altitude bins in a manner similar to the procedure used to compare the profile measurements. There were typically 2–8 level leg comparisons in each altitude bin for each flight, so that there were about 10–30 leg comparisons at each altitude bin above 7 km, for a total of about 60–80 level leg comparisons.

The NASA Langley/Ames DLH is an open-path airborne tunable diode laser-based instrument that operates in the near-infrared spectral region at a wavelength of approximately 1.4 μm (Vay et al. 2000). Diskin et al. (2002) and Podolske et al. (2003) discuss details of instrument operation and calibration; we describe its operation briefly here. The DLH uses an open-path, double-pass configuration, where the path is defined on one end by a laser transceiver mounted on the interior of a modified window panel, and on the other by a panel of retroreflecting material mounted on the DC-8's outboard engine nacelle. Due to the large range of water vapor concentration in the atmosphere from percent-level concentrations at or near sea level to a few parts per million in the lower stratosphere, the DLH operates on one of two spectral absorption lines: a relatively weak line for concentrations above about 100 ppm (~0.06 g kg^{-1}) and a stronger line for concentrations below that level. The weaker line is located at 7121.7 cm^{-1} and is in the (200) vibrational overtone band. The stronger line, which is roughly 10 times stronger than the weaker line, is located at 7117.8 cm^{-1} and is in the (101) combination band. The DLH is calibrated in the laboratory at various combinations of pressure and water vapor density. From the calibration data and a multiparameter spectral model, a set of coefficients is developed, and these coefficients are used to convert the measured signals, along with local temperature and pressure (which are measured by separate instruments aboard the aircraft), to water vapor mixing ratio. The precision of the instrument is 2% of the mixing ratio, with an estimated accuracy of 10% for water vapor above 100 ppmv (Vay et al. 2000). During the Subsonic Assessment Ozone and Nitrogen Oxide Experiment (SONEX) conducted during the fall of 1997, a small (<10 ppm) positive bias was identified during postmission calibrations. The source of this artifact (outgassing within the laser head) was removed for subsequent missions, including AFWEX (Vay et al. 2000). Improved calibration and data analysis procedures and an improved water vapor spectral model have lowered the DLH's errors to less than 5%, or 1 ppmv (Podolske et al. 2003).

Temperature and pressure measurements on the DC-8 were provided by the Data Acquisition and Distribution System (DADS). Temperature was derived from measurements of total air temperature via a Rosemount probe and Mach number from a Collins ADS-85 air data system (ADC). Pressure was calculated from the pressure altitude measured by the ADC. The uncertainties of the temperature and pressure are estimated to be $\pm$1.5 K and $\pm$1 mb, respectively (Vay et al. 2000).

A Buck Research CR1 cryogenic hygrometer (Busen and Buck 1995) was also deployed on the NASA DC-8 aircraft. This instrument, like the Snow White radiosonde sensor, used the chilled-mirror technique to sense the onset of condensation. The mirror temperature,

which is the frost point of the air passing over the mirror, is measured by a thermistor embedded in the mirror. Unlike the Snow White sensor, this instrument uses liquid nitrogen to control the mirror temperature and should permit measurements of low frost points found in the upper troposphere and lower stratosphere. The instrument is capable of measuring frost points down to −80°C with an accuracy to measure the mirror surface temperature to ±0.3°C.

Figure 5b shows a comparison of the DLH and cryogenic water vapor measurements and the LASE measurements. The average differences between the LASE and DLH water vapor measurements varied between ±3% and 8%. The average of all the bias differences was about −3%. The DLH measurements were slightly (4%) drier than the LASE measurements in the upper troposphere. The cryogenic hygrometer measurements became progressively drier with altitude when compared to LASE and the other sensors. The cryogenic hygrometer was about 5% drier than LASE between 7 and 8 km and became up to about 25% drier than LASE at 10–11 km. Note that the cryogenic hygrometer measurements are 5%–20% drier than the DLH measurements. The reasons for this cryogenic hygrometer dry bias are most likely due to physical properties (or restraints) of the chilled-mirror instrument and measurement technique.

Previous comparisons between diode laser hygrometers and frost point hygrometers have also shown the tendency of the cryogenic frost point hygrometers to indicate smaller water vapor amounts than diode laser hygrometers. Schultz et al. (1999) compared the water vapor measurements acquired by these DLH and cryogenic hygrometer sensors during the Pacific Exploratory Mission (PEM) Tropics A campaign; although measurements from both sensors agreed on average to within 20%, for mixing ratios below 100 ppmv (~0.06 g kg^{-1}) the cryogenically cooled mirror tended to be lower by a factor of 2–5. They concluded that the DLH sensor appeared to be more reliable, especially in the upper troposphere. Vay et al. (2000) found that water vapor measurements acquired by a similar cryogenic frost point hygrometer flown on the Falcon aircraft during the Pollution from Aircraft Emissions in the North Atlantic Flight Corridor (POLINAT2) campaign were typically lower than the DLH water vapor measurements. The presence of water vapor within the DLH laser head as discussed above could explain some, but not all, of this difference. Sonnenfroh et al. (1998) also found that cryogenic frost point water vapor measurements were about 20% lower than the diode laser hygrometer water vapor measurements when both instruments were flown on the NASA P-3 aircraft during the Southern Great Plains Hydrology experiment in June 1997. This difference was not understood; however, much better agreement was found when the cryogenic hygrometer water vapor measurements were recomputed assuming the film on the hygrometer mirror was supercooled water instead of frost. For the comparisons above 8 km during AFWEX, temperatures were generally below −30°C so that it is unlikely that the cryogenic hygrometer was sensing supercooled water instead of frost. Diskin et al. (2002) and Podolske et al. (2003) compared these cryogenic hygrometer and DLH measurements with each other and with in situ instruments on board the NASA ER-2 aircraft on a flight during the Stratospheric Aerosol and Gas Experiment (SAGE-III) Ozone Loss and Validation Experiment (SOLVE) mission during January 2000. The ER-2 instruments were the Harvard Lyman-α hygrometer and a diode laser hygrometer developed at the Jet Propulsion Laboratory (JPL) (May et al. 1998). The comparisons, which measured stratospheric water vapor levels of about 10 ppmv (~0.006 g kg^{-1}), showed that the two diode laser hygrometers (NASA Langley and JPL) and the Harvard Lyman-α hygrometer agreed within about 4%, and the cryogenic hygrometer was about 20%–25% lower than these other sensors.

5. Overall comparison

Differences between each sensor's measurements and the LASE measurements were computed every 60 m for altitudes between 7 km and the tropopause and for water vapor mixing ratio values below 0.2 g kg^{-1}. Average bias and rms differences along with the linear regression results corresponding to each comparison with the LASE measurements are listed in Table 2, and the average and standard deviations of these bias differences relative to the LASE measurements are shown in Fig. 9. Comparisons were made in this manner rather than comparing integrated amounts in order to avoid biasing the result to the lowest portion of this altitude region. Note how the overlap correction applied to the CARL water vapor measurements produced better agreement with LASE and the other sensors. Figure 9 also shows that correcting the Vaisala RS80-H radiosondes for bias and time lag errors significantly reduces the upper-troposphere dry bias of these sensors and produces agreement within about 5% with LASE, the Raman lidar measurements, and the in situ DLH measurements on the NASA DC-8 aircraft. Figure 9 shows that Sippican sondes were on average about 15% wetter than the LASE measurements; however, on the basis of these comparisons, these radiosondes exhibited erratic behavior and cannot be expected to provide reliable data in the upper troposphere. The DLH aircraft in situ sensor was about 3%–4% drier than LASE in the upper troposphere. The Snow White chilled-mirror radiosonde and the cryogenic frost point hygrometer measurements were about 10% and 15%–20% lower than the LASE measurements, respectively.

The large standard deviations shown in Figs. 5–7 and 9 are indicative of the large variability among the various comparisons. Much of this variability can be attributed to the large horizontal variability and the dif-

TABLE 2. Linear regression best-fit parameters when comparing water vapor measurements from each sensor to the LASE water vapor measurements. These comparisons were restricted for altitudes between 7 km and the tropopause (~12 km) and for water vapor mixing ratios below 0.2 g kg^{-1}. The total number of points used in the regression analyses is denoted by *N*. For profile comparisons, *N* represents the total number of points used in all the profiles; for the level leg in situ comparisons, *N* represents the number of level leg comparisons; *R* is the linear correlation coefficient; rms is the root-mean-square.

	Slope	Intercept (g kg^{-1})	*N*	*R*	Rms diff (g kg^{-1})	Rms diff (%)	Bias diff (g kg^{-1})	Bias diff (%)
CARL (initial)	1.07	−0.000 76	2423	0.97	0.013	17	0.004 82	6.2
CARL (overlap correction)	1.03	−0.000 73	2423	0.97	0.012	15	0.001 65	2.1
SRL	1.06	−0.002	1550	0.97	0.011	16	0.002 78	4.0
Vaisala (initial)	0.87	0.002	471	0.91	0.018	27	−0.006 82	−10
Vaisala (scaled to MWR PWV)	0.84	0.003	471	0.90	0.018	27	−0.007 84	−12
Vaisala (calibration correction)	0.88	0.003	471	0.91	0.017	25	−0.004 30	−6.2
Vaisala (calibration + time-lag corrections)	0.92	0.004	471	0.92	0.015	22	−0.001 40	−2.0
Chilled-mirror sonde	0.92	−0.000 37	486	0.92	0.020	24	−0.007 37	−8.8
Sippican sonde	1.01	0.011	486	0.80	0.035	48	0.011	15
DLH	0.96	−0.000 89	81	0.96	0.011	19	−0.003 24	−4.0
Cryogenic hygrometer	0.91	−0.005 52	66	0.97	0.014	23	−0.0107	−17

ference in sampling volumes among the various instruments. Examination of the LASE and DLH measurements showed that the water vapor variability (standard deviation/mean) generally ranged from 5% to 30% along the level leg segments of these flights. Large horizontal and vertical water vapor gradients would impact these comparisons due to differences in sampling volumes and vertical resolutions. Recall that the vertical resolution of the LASE measurements is 330 m and that the CARL vertical resolution varies between 300 and 400 m in the upper troposphere. Consequently, comparisons between layer averages from these remote sensors and measurements across a single linear path along a single altitude such as from the DLH can be expected to exhibit large variabilities. Because some of the differences between the instruments are due to these large horizontal and vertical water vapor gradients, the error estimates on these comparisons should represent upper limits on the instrumental differences.

The agreement among LASE, Raman lidars, and Vaisala results indicates that calibrating the Raman lidar to the MWR PWV should provide an accurate method of

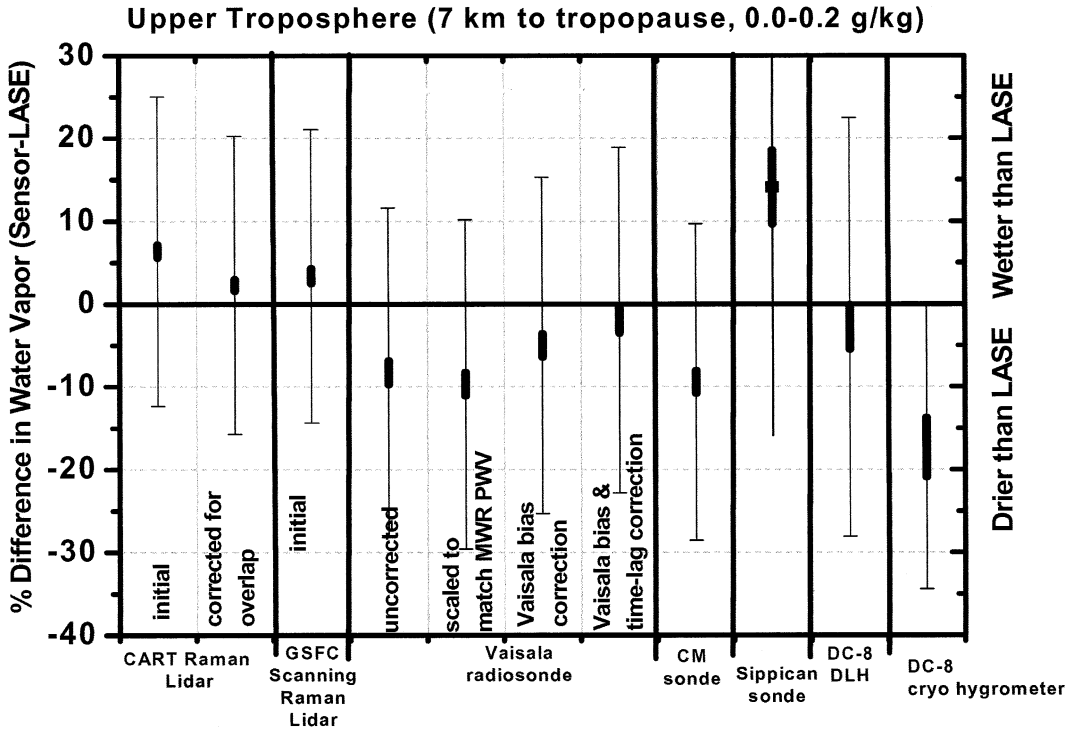

FIG. 9. Average differences between each sensor's UTWV measurements and the LASE UTWV measurements. These differences were computed for altitudes between 7 km and the tropopause (~12 km) and for water vapor mixing ratios between 0 and 0.2 g kg^{-1}.

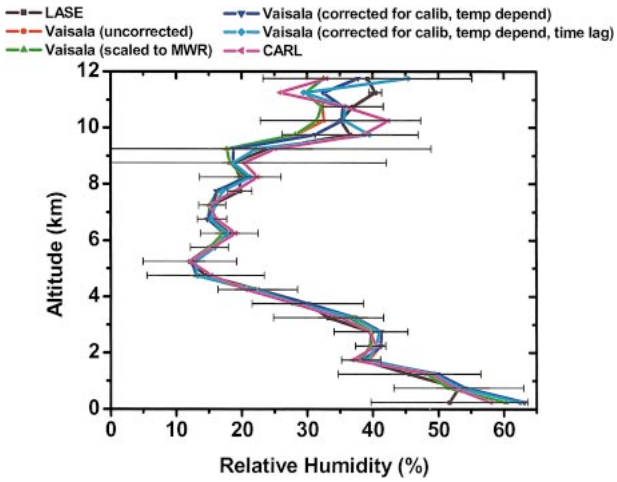

FIG. 10. Average relative humidity profiles from LASE, CARL, and Vaisala radiosonde measurements. The profiles corresponding to the uncorrected and corrected Vaisala profiles are shown. These profiles represent the average of the 16 cases when there were results from LASE, CARL, and all the radiosonde correction procedures. The CARL results include the overlap correction.

retrieving upper-tropospheric water vapor measurements, once appropriate corrections have been applied to the low-altitude Raman lidar water vapor retrievals. These results also show that schemes to correct the dry bias of the Vaisala radiosonde measurements substantially reduce this dry bias and bring these measurements into much better agreement with the lidar and in situ measurements. In contrast, Soden et al. (2004) compared GOES 6.7-μm, CARL, and Vaisala upper-tropospheric water vapor measurements during several IOPs held at the SGP site prior to AFWEX and found that these correction schemes offered little improvement in reducing the Vaisala dry bias. Similar initial comparisons between the GOES and Vaisala UTH performed for AFWEX appear to show a similar behavior, although the corrections appear to be more successful than for the earlier IOPs (B. J. Soden 2003, personal communication). Soden et al. (2004) also compared averaged relative humidity profiles from the original and corrected Vaisala radiosondes and from CARL and found large differences for altitudes above 500 hPa. Figure 10 shows a similar comparison for the 16 cases during AFWEX when there were coincident Vaisala, LASE, and CARL profiles. Average differences among the LASE, CARL, and Vaisala profiles corrected for calibration errors and time lag are generally less than about 5% throughout the entire altitude range and thus do not show the large differences found in this earlier study. The reason for this different behavior may be related to several factors. There is a large uncertainty associated with the contamination correction applied to correct the Vaisala radiosonde profiles acquired during the previous IOPs. The contamination correction typically has much more uncertainty than the corrections for temperature dependence and time lag (Miloshevich et al. 2003). In contrast to these previous IOPs, the Vaisala radiosondes used for AFWEX were new and so were not affected by contamination. The different behavior may also be due to the specific subset of radiosonde profile measurements used in this study as well as the overall humidity profile structure observed during AFWEX. Note also that the previous IOPs were conducted during September when the tropopause heights were higher than during the November–December period for AFWEX. The vertical distribution will have a greater impact on the GOES comparisons, because of the very broad weighting function (~200–600 hPa) of the GOES retrievals. In addition, the simple IR threshold used to screen out cloud contamination in the GOES retrievals may be inadequate to detect very thin clouds such as subvisible cirrus (Soden et al. 2004).

6. Summary and conclusions

This paper has compared upper-tropospheric water vapor measurements acquired over the DOE ARM SGP site in northern Oklahoma during the AFWEX mission in November and December 2000. The water vapor measurements acquired by the LASE airborne DIAL system were used as a reference when comparing water vapor measurements acquired by the DOE ARM SGP CART Raman and NASA GSFC Raman lidars, ARM Vaisala RS80-H radiosondes, Sippican radiosondes, Meteolabor Snow White radiosondes, and in situ cryogenic frost point and diode laser hygrometer (DLH) sensors on the NASA DC-8 aircraft. Since ground-based Raman lidars can obtain upper-tropospheric water vapor measurements only during nighttime operations, all measurements for these comparisons were acquired at night. Seven DC-8 flights were made during 27 November–10 December 2000 over the ARM SGP Central Facility, and LASE collected approximately 26 h of profile data over the SGP using a combination of water vapor absorption cross sections. The DOE ARM CART Raman lidar upper-tropospheric water vapor measurements were initially about 7% wetter than the LASE measurements in the upper troposphere (8–12 km). However, comparisons with instruments on the SGP 60-m tower and radiosondes revealed an altitude dependence of the CARL overlap correction. Modifying this overlap correction slightly to produce better agreement in the lower troposphere reduced the CARL UTWV profiles by about 4% and produced better agreement with LASE and the other sensors. Since the CARL water vapor calibration depends on this overlap correction, accurate upper (and lower) tropospheric water vapor measurements require accurate knowledge of the CARL overlap correction and periodic implementation of appropriate corrections to account for variations to this overlap function. By implementing this correction, the water vapor measurements from LASE and both DOE ARM and GSFC Raman lidars agreed on average within ±5%–6% between the surface and 12 km, which is within the

expected accuracy of the LASE measurements (Browell et al. 1997). Both Raman lidars were calibrated such that the precipitable water vapor (PWV) derived by integrating their water vapor profiles matched the PWV measured by the ARM SGP ground-based microwave radiometer (MWR). PWV derived from the LASE profiles was only slightly greater (~3%) on average than the PWV derived from the ARM SGP microwave radiometer. The agreement between the LASE and MWR PWV and the LASE, SRL, and CARL UTWV measurements supports the hypotheses that MWR measurements of the 22-GHz water vapor line can accurately constrain the total water vapor amount and that the CART Raman lidar, when calibrated using the MWR PWV, can provide an accurate, stable reference for characterizing upper-troposphere water vapor.

Comparisons with the LASE measurements revealed a dry (~10%–20%) bias in the Vaisala RS80-H radiosonde measurements of upper-tropospheric water vapor. This bias increased with altitude and is similar to what has been reported in previous UTWV comparisons. Scaling the Vaisala water vapor profiles such that the radiosonde PWV matches the MWR PWV, which ARM has found to significantly reduce the sonde-to-sonde water vapor variability (Revercomb et al. 2003), did not improve the upper-tropospheric water vapor comparisons. This indicates that additional schemes are required to properly account for the altitude dependence of the radiosonde errors. Portions of a correction scheme developed jointly by NCAR and Vaisala (Wang et al. 2002) were applied to the AFWEX data to account for the error in the basic RS80-H calibration model, and to improve the representation of the temperature dependence of the RS80-H calibration. The AFWEX sondes were new, so no correction was applied to account for possible sensor contamination by outgassing of the plastic packaging material. This scheme reduced the dry bias so that the Vaisala measurements were about 8%–10% drier than the LASE measurements. A correction for the ''time lag'' error that calculates the ambient humidity profile from the measured humidity and temperature profiles based on laboratory measurements of the sensor time constant (63% response time) as a function of temperature (Miloshevich et al. 2001, 2002, 2003, 2004) was found to further reduce the dry bias so that these corrected Vaisala profiles were only 4%–5% drier than the LASE measurements. Using these measurements as a reference, the comparisons shown here indicate that the corrected CARL and Vaisala RS80-H radiosonde profiles are within the ARM goal of 10% in mean differences in UTWV.

Additional studies are desirable to evaluate other upper-tropospheric measurements and resolve remaining differences. Since May 2001, ARM has been using the Vaisala RS90 radiosondes in place of the RS80-H radiosondes. Vaisala RS90 radiosondes were not available for evaluation during AFWEX. Comparisons of uncorrected RS80 and RS90 radiosondes performed by the ARM Program have shown the RS90 radiosondes to be wetter by a few percent in the upper troposphere. This finding is supported by comparisons performed by the WMO Intercomparisons of GPS radiosondes, which found a mean bias of 5% between the uncorrected sondes (RS80 lower). Similarly, Vance et al. (2004) found a similar bias when comparing RS80-H and RS90 radiosondes during the MOTH campaigns. Since the corrections for calibration errors and time lag response tend to moisten the RS80-H measurements in the upper troposphere, this suggests that comparisons of corrected RS80-H and RS90 radiosondes should yield better agreement. Initial comparisons of RS80-H and RS90 radiosondes during the IHOP campaign found systematic differences (Wang et al. 2003), although it is not clear whether these differences are consistent with the results discussed above. The AFWEX results do indicate the need for correcting RS80-H radiosondes to obtain accurate estimates of upper-tropospheric water vapor. Note that methods of correcting individual Vaisala RS80-A and RS90 radiosondes have been implemented for radiosondes launched at the Lindenberg Meteorological Observatory in Germany (Leiterer et al. 1997; Nagel et al. 2001). These corrections require the measurement of sensor-specific parameters prior to each flight and the use of a universal calibration matrix developed for each sensor type. The absolute accuracy of this technique is reported to be $\pm 1\%$ RH (Leiterer et al. 1997; Nagel et al. 2001; Spichtinger et al. 2003).

Interestingly, the upper-troposphere water vapor measurements from the Snow White chilled-mirror radiosondes and the DC-8 in situ frost point hygrometer measurements are lower than the lidar, corrected Vaisala RS80-H, and DC-8 in situ diode laser hygrometer measurements by 5%–10% and 10%–20%, respectively. The reasons for these differences are not clear. Previous comparisons have noted similar tendencies for the aircraft in situ frost point hygrometer to retrieve lower water vapor amounts than the diode laser hygrometers, with differences increasing with colder temperatures. Preliminary comparisons from the IHOP campaign have shown better Snow White chilled-mirror sensor performance than Sippican/VIZ radiosondes and Vaisala RS80-H and RS90s (Wang et al. 2003). However, other comparisons have noted mixed results for upper-tropospheric water vapor measurements with the Snow White measurements under- or overreporting water vapor, especially if very dry layers are encountered (Vömel et al. 2003). Systematic biases have also been found between Vaisala RS90 radiosondes and Snow White radiosondes (Vance et al. 2004). Resolution of these differences may be aided by comparisons of water vapor measurements acquired by the balloon-borne cryogenic frost point hygrometer, such as that developed and used at the NOAA/Climate Monitoring and Diagnostics Laboratory (CMDL). In contrast to the Snow White radiosonde, which uses a Peltier cooler to cool the mirror, the mirror in this instrument is connected to a cryogenic bath.

Overall uncertainty in dewpoint temperature is about 0.5°C in frost point temperature, which is about 10% RH near the tropopause (Vömel et al. 1995). This balloon-borne water vapor sensor has been flown extensively (Oltmans 1985); intercomparisons with stratospheric measurements (Kley et al. 2000) have shown that this sensor is reliable.

Further studies, including intercomparison experiments like AFWEX, are needed to understand, quantify, and hopefully reduce the remaining differences among these sensors. Several of these sensors (e.g., Vaisala RS80-H, RS90, Raman lidars) are currently participating in validation activities associated with the Atmospheric Infrared Sounder (AIRS) sensor on the NASA *Aqua* satellite platform. Using water vapor measurements from these various sensors to validate the upper-tropospheric water vapor measurements derived from the infrared radiances measured by AIRS will require a better understanding of the capabilities and limitations of these sensors. Airborne lidar measurements such as those provided by LASE during AFWEX can be used to help resolve these differences by characterizing upper-tropospheric water vapor and thereby aid satellite validation (Fetzer 2000; Kley et al. 2000) and radiation modeling activities.

Acknowledgments. We thank William Edwards, Leroy Matthews, George Insley, and Jerry Alexander for supporting LASE operations, and Dr. Melody Avery for the DC-8 ozone data, which was used to infer tropospheric heights. The DOE ARM and NASA FIRE programs funded AFWEX. This research was supported by the Office of Biological and Environment Research of the U.S. Department of Energy as part of the Atmospheric Radiation Measurement Program.

REFERENCES

Ackerman, T., and G. Stokes, 2003: The Atmospheric Radiation Measurement Program. *Phys. Today,* **56,** 38–45.

Ansmann, A., M. Riebesell, U. Wandinger, C. Weitkamp, E. Voss, W. Lahmann, and W. Michaelis, 1992: Combined Raman Elastic-Backscatter LIDAR for vertical profiling of moisture, aerosol extinction, backscatter, and LIDAR ratio. *Appl. Phys. B,* **55,** 18–28.

Browell, E. V., 1989: Differential absorption lidar sensing of ozone. *Proc. IEEE,* **77,** 419–432.

——, and S. Ismail, 1995: First lidar measurements of water vapor and aerosols from a high-altitude aircraft. *Proc. Seventh Topical Meeting of the Optical Remote Sensing of the Atmosphere,* Salt Lake City, UT, OSA, 212–214.

——, and Coauthors, 1997: LASE Validation Experiment. *Advances in Atmospheric Remote Sensing with Lidar,* A. Ansmann et al., Eds., Springer-Verlag, 289–295.

——, ——, and R. Ferrare, 2000: Hurricane water vapor, aerosol, and cloud distributions determined from airborne lidar measurements. Preprints, *Symp. on Lidar Atmospheric Monitoring,* Long Beach, CA, Amer. Meteor. Soc., 65–67.

——, and Coauthors, 2001: Large-scale air mass characteristics observed over the remote tropical Pacific Ocean during March–April 1999: Results from PEM Tropics B Field Experiment. *J. Geophys. Res.,* **106** (D23), 32 481–34 502.

Busen, R., and A. L. Buck, 1995: A high-performance hygrometer for aircraft use: Description, installation and flight data. *J. Atmos. Oceanic Technol.,* **12,** 73–84.

Clough, S. A., M. I. Iacono, and J. L. Moncet, 1992: Line-by-line calculations of atmospheric fluxes and cooling rates: Application to water vapor. *J. Geophys. Res.,* **97** (D14), 15 761–15 785.

——, P. D. Brown, J. C. Liljegren, T. R. Shippert, D. D. Turner, R. O. Knuteson, H. E. Revercomb, and W. L. Smith, 1996: Implications for atmospheric state specification from the AERI/LBLRTM quality measurement experiment and the MWR/LBLRTM quality measurement experiment. *Proc. Sixth ARM Science Team Meeting,* San Antonio, TX, U.S. Dept. of Energy, CONF-9603149, 45–49. [Available online at http://www.arm.gov/docs/documents/technical/conf_9603/cloug_96.pdf.]

——, ——, D. D. Turner, T. R. Shippert, J. C. Liljegren, D. C. Tobin, H. E. Revercomb, and R. O. Knuteson, 1999: Effect on the calculated spectral surface radiances due to MWR scaling of sonde water vapor profiles. *Proc. Ninth ARM Science Team Meeting,* San Antonio, TX, U.S. Dept. of Energy, 1–8. [Available online at http://www.arm.gov/docs/documents/technical/conf_9903/clough-99.pdf.]

da Silveira, R. B., G. Fisch, L. A. T. Machado, A. M. Dall' Antonia Jr., L. F. Sapucci, D. Fernandes, and J. Nash, 2003: Executive summary of the WMO intercomparison of GPS radiosondes. WMO Instruments and Observing Methods Rep. 76, WMO/TD 1153, 1–15.

Diskin, G. S., J. R. Podolske, G. W. Sachse, and T. A. Slate, 2002: Open-path airborne tunable diode laser hygrometer. *Proc. SPIE,* **4817,** 132 pp.

DOE, 1990: Atmospheric Radiation Measurement Program Plan. U.S. Department of Energy, DOE/ER-0441, 116 pp.

Ellingson, R. E., 1998: The state of the ARM-IRF accomplishments through 1997. *Proc. Eighth ARM Science Team Meeting,* Tucson, AZ, U.S. Dept. of Energy, DOE/ER-0738, 245–248. [Available online at http://www.arm.gov/docs/documents/technical/conf_9803/ellingson-98.pdf.]

Ferrare, R. A., S. H. Melfi, D. N. Whiteman, K. D. Evans, F. J. Schmidlin, and D.O'C. Starr, 1995: A Comparison of water vapor measurements made by Raman lidar and radiosondes. *J. Atmos. Oceanic Technol.,* **12,** 1177–1195.

——, and Coauthors, 1999: LASE measurements of water vapor, aerosols, and clouds during CAMEX-3. *Proc. Symp. on Optical Remote Sensing of the Atmosphere,* Santa Barbara, CA, OSA, 114–116.

——, and Coauthors, 2000a: Comparison of aerosol optical properties and water vapor among ground and airborne lidars and sun photometers during TARFOX. *J. Geophys. Res.,* **105** (D8), 9917–9933.

——, and Coauthors, 2000b: Comparisons of LASE, aircraft, and satellite measurements of aerosol optical properties and water vapor during TARFOX. *J. Geophys. Res.,* **105** (D8), 9935–9947.

——, and Coauthors, 2002: Characterization of upper troposphere water vapor measurements during AFWEX using LASE. *Proc. 21st Int. Laser Radar Conf.,* Quebec City, Canada, International Coordination-Group for Laser Atmospheric Studies, 397–400.

Fetzer, E., Ed., 2000: AIRS Team Science Validation Plan. Version 2.1.1., JPL D-16822.

Fujiwara, M., M. Shiotani, F. Hasebe, H. Vomel, S. J. Oltmans, and P. Ruppert, 2003: Performance of the Meteolabor ''Snow White'' chilled-mirror hygrometer in the tropical troposphere: Comparison with the Vaisala RS80 A/H-Humicap sensors. *J. Atmos. Oceanic Technol.,* **20,** 1534–1542.

Goff, J. A., and S. Gratch, 1946: Low-pressure properties of water from −160 to 212 F. *Trans. Amer. Soc. Heat. Vent. Eng.,* **52,** 95–122.

Goldsmith, J. E. M., F. H. Blair, S. E. Bisson, and D. D. Turner, 1998: Turn-key Raman lidar for profiling atmospheric water vapor, clouds, and aerosols. *Appl. Opt.,* **37,** 4979–4990.

Grossmann, B., and E. V. Browell, 1989: Spectroscopy of water vapor in the 720-nm wavelength region: Line strengths, self-induced

pressure broadenings and shifts, and temperature dependence of linewidths and shifts. *J. Mol. Spectrosc.*, **136,** 264–294.

Hyland, R. W., and A. Wexler, 1983: Formulations for the thermodynamic properties of the saturated phases of H_2O from 173: 15K to 473.15K. *ASHRAE Trans.*, **89** (2A), 500–519.

Ismail, S., and E. V. Browell, 1989: Airborne and spaceborne lidar measurements of water vapor profiles: A sensitivity analysis. *Appl. Opt.*, **28,** 3603–3615.

——, ——, R. A. Ferrare, S. A. Kooi, M. B. Clayton, V. G. Brackett, and P. B. Russell, 2000: LASE measurements of aerosol and water vapor profiles during TARFOX. *J. Geophys. Res.*, **105** (D8), 9903–9916.

Khvorostyanov, V. I., and K. Sassen, 1998a: Cirrus cloud simulation using explicit microphysics and radiation. Part I: Model description. *J. Atmos. Sci.*, **55,** 1808–1821.

——, and ——, 1998b: Cirrus cloud simulation using explicit microphysics and radiation. Part II: Microphysics, vapor and ice mass budgets, and optical and radiative properties. *J. Atmos. Sci.*, **55,** 1822–1845.

Kley, D., J. M. Russell III, and C. Philips, Eds., 2000: SPARC assessment of upper tropospheric and stratospheric water vapour. WCRP 133, WMO/TD No. 1043, SPARC Rep. 2, 312 pp.

Kooi, S. A., R. A. Ferrare, S. Ismail, E. V. Browell, M. B. Clayton, V. G. Brackett, and J. B. Halverson, 2002: Comparison of LASE water vapor measurements with dropwindsonde measurements during the Third and Fourth Convection and Moisture Experiments (CAMEX-3 and CAMEX-4). *Proc. 21st Int. Laser Radar Conf.,* Quebec City, Canada, International Coordination-Group for Laser Atmospheric Studies, 693–696.

Leiterer, U., H. Dier, and T. Naebert, 1997: Improvements in radiosonde humidity profiles using RS80/RS90 radiosondes of Vaisala. *Beitr. Phys. Atmos.*, **70,** 319–336.

Lesht, B. M., 1995: An evaluation of ARM radiosonde operational performance. Preprints, *Ninth Symp. on Meteorological Observations and Instrumentation,* Charlotte, NC, Amer. Meteor. Soc., 6–10.

——, and J. C. Liljegren, 1996: Comparison of precipitable water vapor measurements obtained by microwave radiometers and radiosondes at the SGP/CART site. *Proc. Sixth ARM Science Team Meeting,* San Antonio, TX, U.S. Dept. of Energy, CONF-9603149, 165–168. [Available online at http://www.arm.gov/docs/documents/technical/conf_9603/lesh_96.pdf.]

Liljegren, J. C., 2000: Automatic self-calibration of the ARM microwave radiometers. *Microwave Radiometry and Remote Sensing of the Environment,* P. Pampaloni, Ed., VSP Press, 433–441. [Available online at http://www.arm.gov/docs/instruments/publications/mwrpcalibration.pdf.]

List, R. J., 1984: *Smithsonian Meteorological Tables.* 5th ed. Smithsonian Institution, 350 pp.

May, R. D., 1998: Open-path, near-infrared tunable diode laser spectrometer for atmospheric measurements of H_2O. *J. Geophys. Res.*, **103,** 19 161–19 172.

Miloshevich, L. M., H. Vomel, A. Paukkunen, A. J. Heymsfield, and S. J. Oltmans, 2001: Characterization and correction of relative humidity measurements from Vaisala RS80-A radiosondes at cold temperatures. *J. Atmos. Oceanic Technol.*, **18,** 135–155.

——, A. Paukkunen, H. Vömel, and S. J. Oltmans, 2002: Impact of Vaisala radiosonde humidity corrections on ARM IOP data. *Proc. 12th ARM Science Team Meeting,* St. Petersburg, FL, U.S. Dept. of Energy, 1–9. [Available online at http://www.arm.gov/docs/documents/technical/conf_0204/miloshevich-lm.pdf.]

——, H. Vömel, S. J. Oltmans, and A. Paukkunen, 2003: In-situ validation of a correction for time-lag and bias errors in Vaisala RS80-H radiosonde humidity measurements. *Proc. 13th ARM Science Team Meeting,* Broomfield, CO, U.S. Dept. of Energy, 1–10. [Available online at http://www.arm.gov/docs/documents/technical/conf_0304/miloshevich-lm.pdf.]

——, A. Paukkunen, H. Vöemel, and S. J. Oltmans, 2004: Development and validation of a time-lag correction for Vaisala radiosonde humidity measurements. *J. Atmos. Oceanic Technol.*, **21,** 1305–1327.

Mlawer, E. J., S. J. Taubman, P. D. Brown, M. J. Iacono, and S. A. Clough, 1997: Radiative transfer for inhomogeneous atmospheres: RRTM, a validated correlated-*k* model for the longwave. *J. Geophys. Res.*, **102,** 16 663–16 682.

Moore, A. S., Jr., and Coauthors, 1997: Development of the Lidar Atmospheric Sensing Experiment (LASE), an advanced airborne DIAL instrument. *Advances in Atmospheric Remote Sensing with Lidar,* A. Ansmann et al., Eds., Springer-Verlag, 281–288.

Nagel, D., U. Leiterer, H. Dier, A. Kats, J. Reichard, and A. Behrendt, 2001: High accuracy humidity measurements using the standardized frequency method with a research upper-air sounding system. *Meteor. Z.*, **10,** 395–405.

NOAA, 1976: *U.S. Standard Atmosphere, 1976,* NOAA-S/T 76-1562, 227 pp.

Oltmans, S. J., 1985: Measurements of water vapor in the stratosphere with a frost point hygrometer. *Proc. 1985 Int. Symp. on Moisture and Humidity,* Washington, DC, Instrument Society of America, 251–258.

Podolske, J. R., G. W. Sachse, and G. S. Diskin, 2003: Calibration and data retrieval algorithms for the NASA Langley/Ames Diode Laser Hygrometer for the NASA Transport and Chemical Evolution Over the Pacific (TRACE-P) mission. *J. Geophys. Res.*, **108,** 8792, doi:10.1029/2002JD003156.

Ponsardin, P. L., and E. V. Browell, 1997: Measurements of $H_2{}^{16}O$ linestrengths and air-induced broadenings and shifts in the 815-nm spectral regions. *J. Mol. Spectrosc.*, **185,** 58–70.

Revercomb, H. E., W. F. Feltz, R. O. Knuteson, D. C. Tobin, P. F. W. van Delst, and B. A. Whitney, 1998: Accomplishments of the Water Vapor IOPs: An overview. *Proc. Eighth ARM Science Team Meeting,* Tucson, AZ, U.S. Department of Energy, DOE/ER-0738, 639–645. [Available online at http://www.arm.gov/docs/documents/technical/conf_9803/revercomb-98.pdf.]

——, and Coauthors, 2003: The Atmospheric Radiation Measurement (ARM) Program's Water Vapor Intensive Observation Periods: Overview, accomplishments, and future challenges. *Bull. Amer. Meteor. Soc.*, **84,** 217–236.

Schermaul, R., R. C. M. Learner, D. A. Nownham, R. G. Williams, J. Ballard, N. F. Zobhov, D. Belmiloud, and J. Tennyson, 2001: The water vapor spectrum in the 8600–15000 cm^{-1}: Experimental and theoretical studies for a new spectral line database. *J. Mol. Spectrosc.*, **208,** 32–42.

Schultz, M. G., and Coauthors, 1999: On the origin of tropospheric ozone and NO_x over the tropical South Pacific. *J. Geophys. Res.*, **104,** 5829–5843.

Sherlock, V., A. Hauchecorne, and J. Lenoble, 1999: Methodology for the independent calibration of Raman backscatter water-vapor lidar systems. *Appl. Opt.*, **38,** 5816–5837.

Shotland, R. M., 1966: Some observations of the vertical profile of water vapor by means of a ground-based optical radar. *Proc. Fourth Symp. on Remote Sensing of Environment,* Ann Arbor, MI, University of Michigan, 273–283.

Smout, R., J. Nash, D. Lyth, and J. Elms, 2002: Comparisons between Vaisala RS90 and Snow White relative humidity measurements from the WMO GPS radiosonde comparison in Brazil (2001) and Ascension Island (1999). *Proc. WMO Tech. Conf. on Meteorological and Environmental Instruments and Methods of Observation (TECO-2002),* Bratislava, Slovak Republic, WMO, Rep. 75, WMO/TD-No. 1123, 1–4.

Soden, B. J., and J. R. Lanzante, 1996: An assessment of satellite and radiosonde climatologies of upper-tropospheric water vapor. *J. Climate,* **9,** 1235–1250.

——, S. A. Ackerman, D. O. Starr, S. H. Melfi, and R. A. Ferrare, 1994: Comparison of upper tropospheric water vapor from GOES, Raman lidar, and cross-chain tracked loran atmospheric sounding system measurements. *J. Geophys. Res.*, **99** (D10), 21 005–21 016.

——, D. D. Turner, B. Lesht, and L. Miloshevich, 2004: An analysis of satellite, radiosonde, and lidar observations of upper tropospheric water vapor from the Atmospheric Radiation Measure-

ment Program. *J. Geophys. Res.,* **109,** D04105, doi:10.1029/2003JD003828.

Sonnenfroh, D. M., W. J. Kessler, J. C. Magill, B. L. Upschulte, M. G. Allen, and J. D. W. Barrick, 1998: In-situ sensing of tropospheric water vapor using an airborne near-IR diode laser hygrometer. *Appl. Phys. B. Laser Opt.,* **67,** 275–282.

Spichtinger, P., K. Gierens, U. Leiterer, and H. Dier, 2003: Ice supersaturation in the tropopause region over Lindenberg, Germany. *Meteor. Z.,* **12** (3), 143–156.

Turner, D. D., and J. E. M. Goldsmith, 1999: Twenty-four-hour Raman lidar water vapor measurements during the Atmospheric Radiation Measurement program's 1996 and 1997 Water Vapor Intensive Observation Periods. *J. Atmos. Oceanic Technol.,* **16,** 1062–1076.

——, R. A. Ferrare, L. A. Heilman, W. F. Feltz, and T. P. Tooman, 2002: Automated retrievals of aerosol extinction coefficient from a Raman lidar. *J. Atmos. Oceanic Technol.,* **19,** 37–50.

——, B. M. Lesht, S. A. Clough, J. C. Liljegren, H. E. Revercomb, and D. C. Tobin, 2003: Dry bias and variability in Vaisala RS80-H radiosondes: The ARM experience. *J. Atmos. Oceanic Technol.,* **20,** 117–132.

——, and Coauthors, 2004: The QME AERI LBLRTM: A closure experiment for downwelling high spectral resolution infrared radiance. *J. Atmos. Sci.,* **61,** 2567–2675.

Vance, A. K., J. P. Taylor, T. J. Hewison, and J. Elms, 2004: Comparison of in situ humidity data from aircraft, dropsonde, and radiosonde. *J. Atmos. Oceanic Technol.,* **21,** 921–932.

Vay, S. A., and Coauthors, 2000: Tropospheric water vapor measurements over the North Atlantic during the Subsonic Assessment Ozone and Nitrogen Oxide Experiment (SONEX). *J. Geophys. Res.,* **105,** 3745–3755.

Vömel, H., S. J. Oltmans, D. J. Hofmann, T. Deshler, and J. M. Rosen, 1995: The evolution of the dehydration in the Antarctic stratospheric vortex. *J. Geophys. Res.,* **100,** 13 919–13 926.

——, M. Fujiwara, M. Shiotani, F. Hasebe, S. J. Oltmans, and J. E. Barnes, 2003: The behavior of the Snow White chilled-mirror hygrometer in very dry conditions. *J. Atmos. Oceanic Technol.,* **20,** 1560–1567.

Wang, J., 2002: Understanding and correcting humidity measurement errors from Vaisala RS80 and VIZ radiosondes. *Proc. Radiosonde Workshop,* Hampton, VA, Hampton University, 1–7.

——, H. L. Cole, D. J. Carlson, E. R. Miller, K. Beierle, A. Paukkunen, and T. K. Laine, 2002: Corrections of humidity measurement errors from the Vaisala RS80 radiosonde—Application to TOGA COARE data. *J. Atmos. Oceanic Technol.,* **19,** 981–1002.

——, D. J. Carlson, D. B. Parsons, T. F. Hock, D. Lauritsen, H. L. Cole, K. Beierle, and E. Chamberlain, 2003: Performance of operational radiosonde humidity sensors in direct comparison with a chilled mirror dew-point hygrometer and its climate implication. *Geophys. Res. Lett.,* **30,** 1860, doi:10.1029/2003GL016985.

Whiteman, D. N., 2003a: Examination of the traditional Raman lidar technique. I. Evaluating the temperature-dependent lidar equations. *Appl. Opt.,* **42,** 2571–2592.

——, 2003b: Examination of the traditional Raman lidar technique. II. Evaluating the ratios for water vapor and aerosols. *Appl. Opt.,* **42,** 2593–2605.

——, and S. H. Melfi, 1999: Cloud liquid water, mean droplet radius, and number density measurements using a Raman lidar. *J. Geophys. Res.,* **104,** 31 411–31 419.

——, ——, and R. A. Ferrare, 1992: Raman lidar system for the measurement of water vapor and aerosols in the earth's atmosphere. *Appl. Opt.,* **31,** 3068–3082.

——, and Coauthors, 2001a: 2001: NASA/GSFC scanning Raman lidar participation in WVIOP2000 and AFWEX. *Proc. 11th ARM Science Team Meeting,* Atlanta, GA, U.S. Dept. of Energy, 1–10. [Available online at http://www.arm.gov/docs/documents/technical/conf_0103/whiteman-dn.pdf.]

——, and Coauthors, 2001b: Raman lidar measurements of water vapor and cirrus clouds during the passage of Hurricane Bonnie. *J. Geophys. Res.,* **106** (D6), 5211–5225.

——, K. Evans, B. Demoz, P. Di Girolamo, B. Mielke, and B. Stein, 2002: Advances in Raman lidar measurements of water vapor. *Proc. 21st Int. Laser Radar Conf.,* Quebec, QC, Canada, International Coordination-Group for Laser Atmospheric Studies, 551–554.